

Correlation of hole mobility, exciton diffusion length, and solar cell characteristics in phthalocyanine / fullerene organic solar cells<sup>(a)</sup>

寺尾 佑生, 雀部 博之, 安達 千波矢

Yuhki Terao, Hiroyuki Sasabe, Chihaya Adachi

**要旨** 金属フタロシアニン (MPc,  $M = \text{Fe, Co, Ni, Cu, Zn}$  and  $\text{H}_2$ ) およびフラーレン ( $\text{C}_{60}$ ) を積層させたヘテロ接合型有機太陽電池において, MPc のホール移動度および励起子拡散長を太陽電池特性と比較した。その結果, ZnPc を除く MPc を用いた太陽電池では短絡電流がホール移動度と線形関係を示した。また, それぞれの MPc について励起子拡散長を理論計算によって求めたところ, 励起子拡散長は短絡電流と比例関係を示し, 両者が強い相関関係にあることが確認された。

**Abstract** The authors investigated heterojunction organic solar cells composed of different metal phthalocyanines (MPcs,  $M = \text{Fe, Co, Ni, Cu, and H}_2$ )/fullerene ( $\text{C}_{60}$ ) and compared the solar cell characteristics with the field-effect hole mobilities ( $\mu_h$ ) and exciton diffusion length ( $L_{\text{ex}}$ ) of the different MPcs. They observed that the short circuit current ( $J_{\text{SC}}$ ) is linearly dependent on the  $\mu_h$  of the MPcs, except for ZnPc. They also estimated the  $L_{\text{ex}}$  of the MPcs by creating a line of best fit using the action spectra of the external quantum efficiency in the solar cells and found that  $J_{\text{SC}}$  is closely correlated with the  $L_{\text{ex}}$  of the MPcs.

**キーワード** : 有機太陽電池, 金属フタロシアニン, 短絡電流, ホール移動度, 励起子拡散長

**Keywords** : Organic photovoltaic, Metal phthalocyanine, Short circuit current, Hole mobility, Exciton diffusion length

Organic solar cells (OSCs) have recently been proposed as a key for energy supply because they cover a large area, are inexpensive and produce flexible solar cells. By incorporating multilayers<sup>(1)</sup> and bulk heterojunctions<sup>(2)</sup>, the energy conversion efficiency ( $\eta_p$ ) of OSCs was gradually increased  $\sim 5\%$ <sup>(3)</sup>. However, the  $\eta_p$  is still low for practical applications and has been anticipated to clarify the controlling factors required to obtain a higher conversion efficiency. Also, since only a limited number of organic materials can function in OSCs, establishing more effective material designs and expanding the number of materials required to produce OSCs are needed. In photovoltaic processes, solar cell characteristics are expected to have strong correlation with not only the carrier transport but

also exciton diffusion. Since only excitons that reach a donor-acceptor interface, i.e., a  $p$ - $n$  heterojunction interface, are dissociated into holes and electrons, a longer exciton diffusion length can contribute to generating more charge carriers<sup>(4)</sup>. Further, the dissociated holes and electrons have to move to opposite electrodes by using an internal built-in electric field. Therefore, organic materials having a long exciton diffusion length ( $L_{\text{ex}}$ ) and high carrier mobility ( $\mu$ ) are desirable for improving the  $\eta_p$ . Since the  $\mu$  and  $L_{\text{ex}}$  are strongly dependent on the molecular stacking, a high  $\mu$  generally could cause a long  $L_{\text{ex}}$ . In fact, a high  $\eta_p$  has recently been achieved by using pentacene<sup>(5)</sup> and tetracene<sup>(6)</sup> as a  $p$ -type semiconductor and fullerene ( $\text{C}_{60}$ ) (Ref.7) as an  $n$ -type semiconductor. These materials are known to have

(a) 本論文は Applied Physics Letters, Volume 90, 103515 (2007 年) に発表済みであり, American Institute of Physics より転載許可を得ている。

high carrier mobility and a rather large  $L_{ex}$  due to their high molecular packing nature<sup>(8)-(10)</sup>.

In this work, we fabricated heterojunction OSCs having different metal phthalocyanines (*MPcs*) as a *p*-type semiconductor and  $C_{60}$  as an *n*-type semiconductor and compared their solar cell characteristics with the hole mobility ( $\mu_h$ ) and  $L_{ex}$  of the *MPcs*. To date, the *MPcs* have been widely used in *p*-type semiconductor layers in OSCs, and in this experiment, we used six Pc derivatives: FePc, CoPc, NiPc, CuPc, ZnPc, and metal-free phthalocyanine ( $H_2Pc$ ). The CuPc,  $H_2Pc$  and ZnPc derivatives are well established as *p*-type semiconductors in OSCs<sup>(11)-(13)</sup>, and the FePc, CoPc, and NiPc derivatives were used for comparison. The central metals of *MPcs* the Fe, Co, Ni, Cu, and Zn, are transition metals, and they all have different magnetic properties derived from the *3d* orbital. Therefore, the *MPcs* have different molecular orbital levels, but the atomic radii and the weights of the central metals are quite similar<sup>(14)</sup>.

The OSCs were fabricated on a pre-cleaned indium tin oxide (ITO)-coated glass substrate. The organic layers were grown by using thermal evaporation in a vacuum less than  $3 \times 10^{-3}$  Pa. Before the organic layers were deposited, all *MPcs* were purified more than two times by using thermal gradient train sublimation<sup>(15)</sup>. We used  $C_{60}$  (Frontier Carbon Corp.) as received, and no further purification was performed. A 40-nm-thick *MPcs* layer was deposited on the substrate, followed by a 30-nm-thick  $C_{60}$  layer as the *n*-type semiconductor and a 10-nm-thick bathocuproine (BCP)

layer to block excitons. A 50-nm-thick Ag film was then deposited through a shadow mask to define a circle-shaped active area with a diameter of 500  $\mu m$ . After deposition, we measured the current density-voltage (*J-V*) characteristics using a source-measurement system (Advantest R6243) under AM1.5G illumination with a power of 100 mW/cm<sup>2</sup> produced by a solar simulator (Oriel 66901).

Organic field-effect transistor structures were also fabricated by depositing *MPcs* on a Si/SiO<sub>2</sub>(300nm) substrate having comb-type electrodes composed of Cr (1nm)/Au (40nm) on the surface. The channel length and width were 25  $\mu m$  and 4 mm, respectively, for 19 pairs. Before the *MPcs* were deposited, the Si substrates were cleaned by using acetone in an ultrasonic cleaner and by boiling them in isopropanol, and were then coated with 1,1,1,3,3,3-hexamethyldisilazane as a hydrophobic layer. After fabrication, we immediately measured the drain current-voltage ( $I_D$ - $V_D$ ) characteristics using a semiconductor parameter analyzer (Agilent 4155C) in a vacuum less than  $1 \times 10^{-2}$  Pa.

Figure 1(a) shows the *J-V* characteristics of OSCs using different *MPcs*, and Table I lists the OSC characteristics. Each OSC showed clear photovoltaic characteristics, i.e., open circuit voltage ( $V_{oc}$ ), short circuit current ( $J_{sc}$ ), and fill factor (FF), demonstrating that  $\eta_p$  is apparently dependent on *MPcs*, ranging from 0.019% to 1.1%.

First, we will discuss the *MPcs*' dependence on  $J_{sc}$ . The origins of the  $J_{sc}$  are rather complicated because the  $J_{sc}$  is

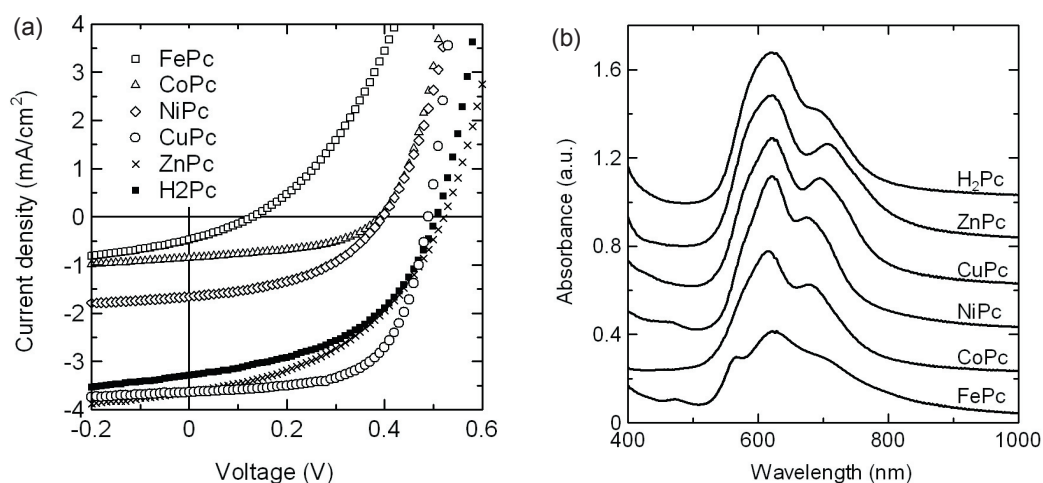


FIG. 1 (a) Current density (*J*) – voltage (*V*) characteristics in solar cells with different metal phthalocyanines (*MPcs*). (b) Absorption spectra of FePc, CoPc, NiPc, CuPc, ZnPc, and  $H_2Pc$  deposited films with thickness of 100 nm.

determined by various factors: (i) the absorption coefficient of the organic layers, (ii) the effective area of the  $p$ - $n$  junction, (iii) the absorbed light intensity distribution inside the cell, (iv) the diffusion efficiency of the excitons, (v) the transport efficiency of the charge carriers, and (vi) the collecting efficiency of the charge carriers. The absorption intensities of the  $MPc$ s are corrected depending on the absorption spectra, as shown in Fig. 1(b). Second, we can assume that the  $p$ - $n$  junction width in each cell is the same. Third, since the imaginary refraction indices of the  $MPc$ s are similar in these derivative<sup>(16),(17)</sup>, the absorbed light intensity distribution can be assumed to be the same. Fourth, since the difference of the highest occupied molecular orbital (HOMO) levels between the  $MPc$ s is so small, as listed in Table I, and the energy barriers between the ITO anode and  $MPc$ s are comparable, we can neglect the correcting efficiency of holes at the interfaces between  $MPc$ s and the

anode. After all, the  $J_{SC}$  can be controlled by the factors of the diffusion efficiency of the excitons (iv) and the transport efficiency of the charge carriers (v). As  $J_{SC}$  is the sum of  $J_h + J_e$ , where  $J_h$  is the hole current and  $J_e$  is the electron current, we can assume that  $J_e$  is independent of the type of  $MPc$ s. Thus,  $J_h$  and  $J_{SC}$  can be expressed by using the linear sum of the drift current and the diffusion current,

$$J_h = n_h \mu_h \nabla U + kT \mu_h \nabla n_h, \quad (1)$$

$$J_{SC} = J_h + J_e, \quad (2)$$

where  $n_h$  is the concentration of holes,  $U$  is the electrical potential,  $k$  is Boltzmann's constant, and  $T$  is the temperature. Based on Eqs. (1) and (2),  $J_{SC}$  is proportional to  $\mu_h$ . Therefore,  $J_{SC}$  can be primarily controlled by carrier mobility, i.e., the  $\mu_h$ , of the  $MPc$ s in these devices.

Figure 2(a) shows a comparison of the  $J_{SC}$  and the  $\mu_h$  of the  $MPc$ s obtained by using their FET characteristics.

TABLE I Summary of OSC characteristics having different  $MPc$ s as a  $p$ -type semiconductor layer, HOMO/LUMO levels of  $MPc$ s, and the  $L_{MPc}$  and  $\eta_{CMPc}$  that we estimated.

$MPc$	$\eta_p$ (%)	$V_{OC}$ (V)	$J_{SC}$ (mA/cm <sup>2</sup> )	FF (%)	HOMO/LUMO (eV)	$L_{MPc}$ (nm)	$\eta_{CMPc}$
	0.019	0.13	0.48	30	4.78 / 3.32	1.0	0.14
CoPc	0.16	0.39	0.85	48	4.93 / 3.37	1.6	0.17
NiPc	0.30	0.40	1.7	45	4.68 / 3.44	9.0	0.21
CuPc	1.1	0.49	3.6	62	4.82 / 3.13	15.4	0.33
ZnPc	0.84	0.52	3.6	44	4.75 / 3.28	15.0	0.33
H <sub>2</sub> Pc	0.80	0.51	3.3	48	4.86 / 3.21	11.9	0.34

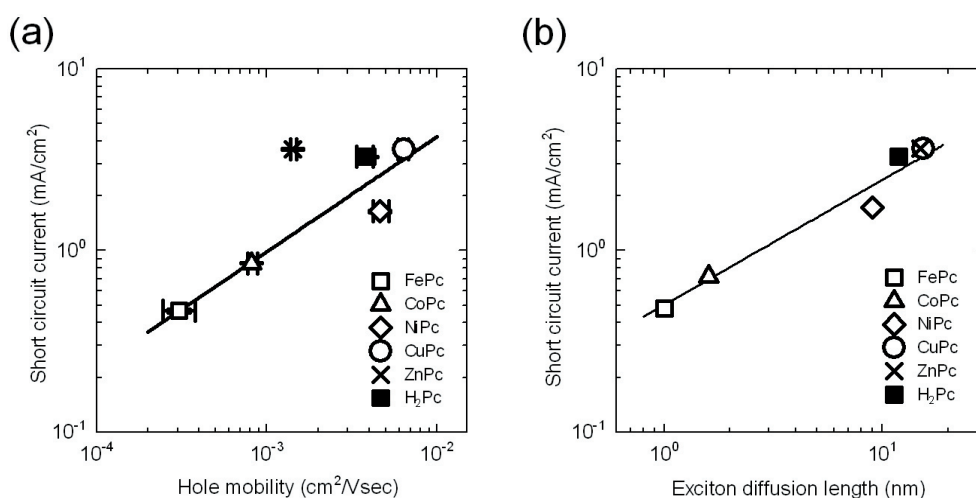


FIG. 2 (a)  $J_{SC}$  vs field effect hole mobility of metal phthalocyanines. The solid line is linearly fitted, except for ZnPc. (b)  $J_{SC}$  vs exciton diffusion length of  $MPc$ s.

We found that the  $J_{SC}$  has a rather good linear relationship with the field effect  $\mu_h$ , except for ZnPc. The ZnPc showed a large deviation from the linear relationship, suggesting the presence of other controlling factors in the  $J$ - $V$  characteristics.

Next, we will discuss the exciton diffusion length of the  $MPc$ s. Since charge carriers can be generated from exciton dissociation in the OSCs<sup>(18)</sup>, the exciton diffusion can significantly influence the carrier-generation process in the OSCs. Measuring the exciton diffusion length of  $MPc$ s directly is difficult because there is no photoluminescence in the  $MPc$ s' neat films. Therefore, we estimated the exciton diffusion length using the action spectra of the external quantum efficiency (EQE) in the OSCs. The EQE is defined as the ratio of the number of collected carriers to the number of incident photons and is expressed as follows:

$$EQE(\lambda) = \frac{hc}{e\lambda} \cdot \frac{J_{SC}(\lambda)}{P_{ph}(\lambda)}, \quad (3)$$

where  $h$  is Planck's constant,  $c$  is the speed of light,  $e$  is the elementary electric charge,  $\lambda$  is the wavelength, and  $P_{ph}$  is the power of incident light. In the EQE action spectra shown in Fig. 3(a), two broad peaks due to  $MPc$  and  $C_{60}$  can be identified. In the long-wavelength component longer than  $\lambda \sim 550$  nm, which originates from the  $MPc$  absorption, the EQE showed a large difference, while the absorption spectra of  $MPc$ s are quite similar.

When estimating the exciton diffusion length, we considered that excitons should follow the steady state diffusion equation as follows<sup>(19)</sup>:

$$L_j^2 \frac{\partial^2 n_j(x)}{\partial x^2} - n_j(x) + \tau_j \cdot \frac{Q_j(x)}{hc/\lambda} = 0, \quad (4)$$

where  $L_j$  is the diffusion length of excitons,  $n_j(x)$  is the density of excitons,  $\tau_j$  is the lifetime of excitons, and  $Q_j(x)$  is the time-averaged absorbed optical energy. Suffix  $j$  indicates an organic layer, e.g.,  $n_{MPc}$  and  $n_{C_{60}}$  are the exciton densities inside the  $MPc$  and  $C_{60}$  layer. The  $Q_j(x)$  is proportional to the  $|E(x)|^2$ <sup>(19)</sup>, where  $E(x)$  is the optical electric field that can be calculated by using the transfer matrix method. In solving diffusion equation [Eq. (4)], we assumed an  $n_j$  of zero at the  $p$ - $n$  junction interface and an  $\partial n_j / \partial x$  of zero at the ITO/ $MPc$  and  $C_{60}$ /BCP interface as the boundary conditions. Although the  $MPc$  and  $C_{60}$  interface may be inhomogeneous due to the diffusion of both materials, we assumed the clear interface as a first approximation in Eq. (5). Consequently, we can obtain the density of excitons that reach the  $p$ - $n$  junction, using the following equation:

$$n_j(x_0) = \frac{L_j^2}{\tau_j} \left. \frac{\partial n_j(x)}{\partial x} \right|_{x=x_0}, \quad (5)$$

where  $x_0$  is the position of the  $p$ - $n$  junction. We assumed that the excitons that arrive at the  $p$ - $n$  junction are dissociated

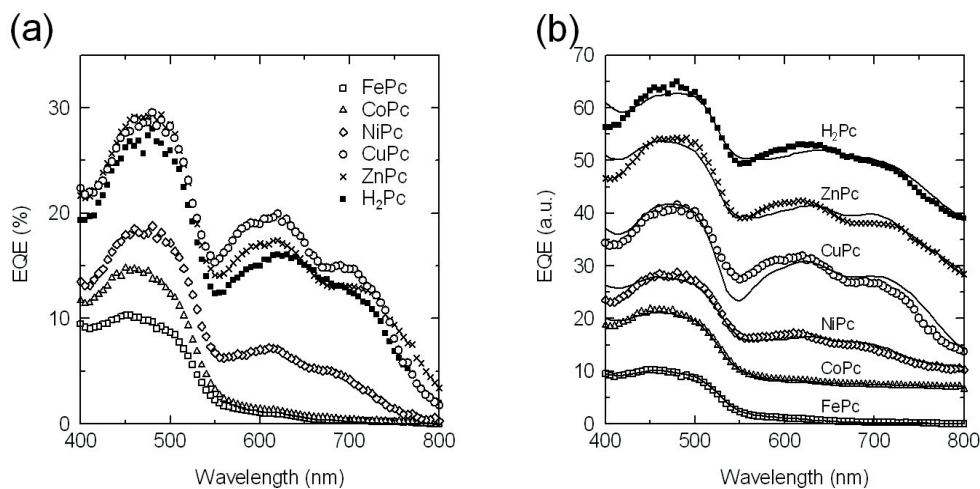


FIG. 3 (a) Action spectra of external quantum efficiency (EQE) in solar cells with  $MPc$ s. (b) Experimental and calculated EQE action spectra in solar cells using  $MPc$ s. The solid lines are calculated EQEs. Exciton diffusion lengths of  $MPc$ s determined by best fitting are  $L_{FePc}$  of 1.0 nm,  $L_{CoPc}$  of 1.4 nm,  $L_{NiPc}$  of 9.1 nm,  $L_{CuPc}$  of 15.7 nm,  $L_{ZnPc}$  of 14.7 nm, and  $L_{H2Pc}$  of 11.9 nm.

into holes and electrons with the probability of  $\eta_{ED}$ . In addition, since a great number of holes and electrons accumulate near the interface, we should consider the recombination probability,  $\eta_R$ . Therefore, the number of holes and electrons contributing to  $J_{SC}$  is expressed as follows:

$$n_{CC} = \eta_{ED} \eta_R (n_{MPc} + n_{C_{60}}) = \eta_C (n_{MPc} + n_{C_{60}}), \quad (6)$$

where  $n_{CC}$  is the number of photo induced charge carriers, and  $\eta_C$  is the exciton-to-charge carrier conversion efficiency, defined as  $\eta_C = \eta_{ED} \eta_R$ . Since  $\eta_{ED}$  and  $\eta_R$  depend on the combination of the donor and acceptor materials, we can assume that  $\eta_C$  depends on  $MPc$ , and  $\eta_C$  can be described as  $\eta_{MPc}$ . We assumed that all the photo generated charge carriers are collected at the anode and the cathode. The EQE is defined as  $n_{CC}$  normalized by the number of incident photons. Therefore, the EQE consists of  $L_{MPc}$ ,  $L_{C_{60}}$ , and  $\eta_{MPc}$ . We fitted the calculated EQE to the experimental data by varying both the  $L_{MPc}$  and  $\eta_{MPc}$ , as shown in Fig. 3(b), where a  $L_{C_{60}}$  of 40 nm was assumed<sup>(4)</sup>. As the result, we obtained  $\eta_{MPc}$  and  $\eta_{C_{60}}$ , as shown in Table I. Based on these estimations, we found an almost linear correlation between  $J_{SC}$  and  $L_{MPc}$ , as shown in Fig. 2(b). All  $MPc$ s fall along the line of best fit, i.e., strongly suggesting that the exciton diffusion length of the  $MPc$ s controls the  $J$ - $V$  characteristics of the OSCs. Therefore, we can expect that the OSC characteristics can enhance a considerably higher  $\eta_P$  by using organic semiconductor materials with a long  $L_{ex}$ .

We found that the  $V_{OC}$  and FF also tend to increase with  $\mu_h$ . The maximum  $V_{OC}$  of 0.52 V in ZnPc is four times larger than that of the minimum  $V_{OC}$  of 0.13 V in FePc. There is no straightforward correlation between the  $V_{OC}$  and the energy gap between the lowest unoccupied molecular orbital (LUMO) level of the acceptor ( $C_{60}$ ) and the HOMO level of the donor ( $MPc$ s) since the differences in the HOMO levels of the  $MPc$ s are much smaller than those of  $V_{OC}$ . Gregg and Hanna proposed that the  $V_{OC}$  is controlled by a chemical potential gradient of the OSCs<sup>(18)</sup>. The chemical potential gradient is equivalent to the carrier density gradient and would depend on the carrier mobility. Based on this idea,  $V_{OC}$  is dependent on  $\mu_h$ .

## References

- (1) C. W. Tang, Appl. Phys. Lett. **48**, 183 (1986).
- (2) M. Hiramoto, H. Fujiwara, and M. Yokoyama, Appl. Phys. Lett. **58**, 1062 (1991).
- (3) J. Xue, S. Uchida, B. P. Rand, and S. R. Forrest, Appl. Phys. Lett. **85**, 5757 (2004).
- (4) P. Peumans, A. Yakimov, and S. R. Forrest, J. Appl. Phys. **93**, 3693 (2003).
- (5) S. Yoo, B. Domercq, and B. Kippelen, Appl. Phys. Lett. **85**, 5427 (2004).
- (6) C. W. Chu, Y. Shao, V. Shrotriya, and Y. Yang, Appl. Phys. Lett. **86**, 243506 (2005).
- (7) P. Peumans and S. R. Forrest, Appl. Phys. Lett. **79**, 126 (2001).
- (8) O. D. Jurchescu, J. Baas, and T. T. M. Palstra, Appl. Phys. Lett. **84**, 3061 (2004).
- (9) R. W. I. de Boer, T. M. Klapwijk, and A. F. Morpurgo, Appl. Phys. Lett. **83**, 4345 (2003).
- (10) Y. Kubozono, T. Nagano, Y. Haruyama, E. Kuwahara, T. Takayanagi, K. Ochi, and A. Fujiwara, Appl. Phys. Lett. **87**, 143506 (2005).
- (11) J. Xue, S. Uchida, B. P. Rand, and S. R. Forrest, Appl. Phys. Lett. **84**, 3013 (2004).
- (12) T. Taima, M. Chikamatsu, Y. Yoshida, K. Saito, and K. Yase, Appl. Phys. Lett. **85**, 6412 (2004).
- (13) K. Suemori, T. Miyata, M. Yokoyama, and M. Hiramoto, Appl. Phys. Lett. **86**, 063509 (2005).
- (14) M-S. Liao and S. Scheiner, J. Chem. Phys. **114**, 9780 (2001).
- (15) H.J. Wagner, R.O. Loutfy and C.K. Hsiao, J. Mater. Sci., **17**, 17 (1982).
- (16) Z. T. Liu, H. S. Kwok, and A. B. Djuricic, J. Phys. D **37**, 678 (2004).
- (17) O. D. Gordan, M. Friedrich, and D. R. T. Zahn, Thin Solid Films **455/456**, 551 (2004).
- (18) B. A. Gregg and M. C. Hanna, J. Appl. Phys. **93**, 3605 (2003).
- (19) L. A. A. Pettersson, L. S. Roman, and O. Inganäs, J. Appl. Phys. **86**, 487 (1999).

## 筆者紹介

寺尾 佑生 (てらお ゆうき)

技術開発本部 総合研究所 デバイス研究センター 表示デバイス研究部。有機 EL の開発を経て、現在有機太陽電池の研究開発に従事。

雀部 博之 (ささべ ひろゆき)

- 1966年: 東京大学大学院 工学系研究科 応用物理学 修士課程修了
- 1966年: 通商産業省 工業技術院 電気試験所 (現・産業技術総合研究所) 研究官 / 主任研究官
- 1974年: 東京農工大学 工学部 電子工学科 助教授
- 1983年: 理化学研究所 生体高分子物理研究室 主任研究員
- 1999年: 千歳科学技術大学 光科学部 物質光科学科 教授
- 2002年: 千歳科学技術大学 学長

安達 千波矢 (あだち ちはや)

- 1991年: 九州大学 大学院 総合理工学研究科 博士課程修了 (工学博士)
- 1991年: (株) リコー 化成品技術研究所 研究員
- 1996年: 信州大学 繊維学部 機能高分子学科 助手
- 1999年: プリンストン大学 Center for Photonics and Optoelectronic Materials 研究員
- 2001年: 千歳科学技術大学 光科学部 物質光科学科 助教授
- 2004年: 千歳科学技術大学 光科学部 物質光科学科 教授
- 2005年: 九州大学 未来化学創造センター 教授